Degenerate four-wave-mixing signals from a dc- and ac-driven semiconductor superlattice

Ren-Bao Liu* and Bang-Fen Zhu
National Lab for Superlattices and Microstructures, Institute of Semiconductors, Chinese Academy of Sciences, P.O. Box 912, Beijing 100 083, People's Republic of China
(Received 29 July 1998)

Within the one-dimensional tight-binding model and χ-3 approximation, we have calculated four-wave-mixing (FWM) signals for a semiconductor superlattice in the presence of both static and high-frequency electric fields. When the exciton effect is negligible, the time-periodic field dynamically delocalizes the otherwise localized Wannier-Stark states, and accordingly quasienergy band structures are formed, and manifest in the FWM spectra as a series of equally separated continua. The width of each continuum is proportional to the joint width of the valence and conduction minibands and is independent of the Wannier-Stark index. The realistic homogeneous broadening blurs the continua into broad peaks, whose line shapes, far from the Lorentzian, vary with the delay time in the FWM spectra. The swinging range of the peaks is just the quasienergy bandwidth. The dynamical delocalization (DDL) also induces significant FWM signals well beyond the excitation energy window. When the Coulomb interaction is taken into account, the unequal spacing between the excitonic Wannier-Stark levels weakens the DDL effect, and the FWM spectrum is transformed into groups of discrete lines. Strikingly, the groups are evenly spaced by the ac field frequency, reflecting the characteristic of the quasienergy states. The homogeneous broadening again smears out the line structures, leading to the excitonic FWM spectra quite similar to those without the exciton effect. However, all these features predicted by the dynamical theory do not appear in a recent experiment [Phys. Rev. Lett. **79**, 301 (1997)], in which, by using the static approximation the observed Wannier-Stark ladder with delay-time-dependent spacing in the FWM spectra is attributed to a temporally periodic dipole field, produced by the Bloch oscillation of electrons in real space. The contradiction between the dynamical theory and the experiments is discussed. In addition, our calculation indicates that the dynamical localization coherently enhances the time-integrated FWM signals. The feasibility of using such a technique to study the dynamical localization phenomena is shown.
[S0163-1829(99)10607-6]

I. INTRODUCTION

It was predicted more than half a century ago that Bloch electrons accelerated by a uniform static field[1] would oscillate in both real and momentum space. The Bloch oscillation (BO),[2] as it was later named, is characterized by a time period

$$\tau_{BO}=\frac{2\pi}{\omega_{BO}}=\frac{h}{eFd} \tag{1}$$

and a spatial amplitude

$$L=\frac{\Delta}{2eF}, \tag{2}$$

where F represents the field strength, d is the lattice period, and Δ is the bandwidth. This temporally periodic movement has its frequency counterpart, i.e., the Wannier-Stark state, which is designated by a Wannier-Stark index n with the energy

$$E_n=E_0+neFd \quad (n=0,\pm 1,\pm 2,\ldots). \tag{3}$$

Because of the equal energy separation, these Wannier-Stark states form the Wannier-Stark ladder (WSL).[3]

The existence of the WSL and BO, however, had been controversial,[4,5] until recently they were confirmed by a number of experiments.[6–14] The key to success in these experiments is the application of semiconductor superlattices,[15] where the long period of the artificial lattice makes τ_{BO} shorter than the dephasing time of carriers under a moderate applied field.

The gedanken experiment to observe BO is to prepare an electron wave packet at momentum k and trace its movement after the field is switched on, but this seems inaccessible. The experiments so far usually involve interband excitations, which are complicated by the hole dynamics and exciton effects. The first two successful experiments in this field were the observation of equally spaced WSL's in superlattices with cw excitations.[6,7] Later, in time-resolved experiments, coherent BO and WSL's have been observed by using the four-wave-mixing (FWM) technique,[8,9] and confirmed by the THz radiation detection.[10,11] The measured BO period and WSL spacing agree well with Eqs. (1) and (3), respectively, if the excitonic modifications are taken into proper account.[16] Recently, an inverse THz experiment detected the BO,[12] and two remarkable experiments demonstrated the WSL and BO in a lattice of atoms in a trap and measured the atomic k-space distribution.[13,14]

All these experiments, however, did not directly measure the spatial amplitude of the Bloch oscillation. Quantum calculations show that the spatial oscillation amplitude of an excited wave packet may differ significantly from the semiclassical result given by Eq. (2) under certain excitation condition.[17–19] For instance, the wave packet may move in a breathing mode, with no center-of-mass motion. Thus, it is

 ©1999 The American Physical Society

of interest and importance to detect the spatial amplitude of the BO directly. Such a measurement was claimed very recently by Lyssenko *et al.*[20] The principle of this experiment is as follows. In suitable excitation, the oscillating dipoles may accompany the excited moving electrons, and opposite charges may be accumulated on the edges of a finite superlattice. Thus a temporally oscillating dipole field is created, which is directly related to the BO of wave packets. The authors have taken the static approximation in dealing with the effect of the dipole field on the WSL. That is, let $F_1(t)$ be the weak dipole field and F the applied static field, in the static approximation used in Ref. 20, the time-dependent field $F+F_1(t)$ leads directly to a dynamical WSL through Eq. (3), and correspondingly to oscillating peaks in FWM spectra. Such fluctuations were traced carefully to follow the dipole field and in turn the spatial displacement of electrons, with the relation between the peak shift ΔE_n with the nth Wannier-Stark level and the displacement $z(t)$ as

$$\Delta E_n=\frac{4\pi n e^2 n_{well}}{\epsilon_r}z(t), \tag{4}$$

where n_{well} is the excited e-h pair density per well, and ϵ_r is the relative dielectric constant of the material. In the experiment, swinging peak positions are observed in FWM spectra as functions of the delay time between the two pulses, which have been attributed by the authors to the real-time-dependent dipole field caused by the BO.

In the static approximation, the time-dependent field is treated as a quasistatic one; that is, the WSL is not affected by the ac field except that the spacing becomes delay time dependent.[20] Consequently, (a) the peak associated with the Wannier-Stark level of the index 0 does not shift with the delay time; (b) peaks with opposite indices move oppositely; and (c) the swinging amplitude of each peak is proportional to the Wannier-Stark index, and independent of the combined electron-hole miniband width. Since these features were observed,[20] the authors thus claimed the detection of the time-periodic dipole field and the spatial BO of electrons.

In our opinion, whether or not a time-dependent field can be treated as a static one relies on its frequency but not on the field strength. If an ac field varies slowly compared to the BO, the static approximation is acceptable. However, the dipole field associated with the BO should vary as quickly like the BO itself, and its influence on the BO or the WSL has to be considered in a full dynamical model.

A number of authors researched the behavior of a lattice of electrons in the presence of both static and high-frequency fields (for a review, see, e.g., Ref. 21), and obtained many fascinating results,[22–28] such as dynamical delocalization (DDL) and dynamical localization (DL), self-transparency, absolute negative conductivity, photon-assisted domain and tunneling, fractional Wannier-Stark ladders, etc. When a Bloch electron is driven by a temporally periodic field,[23–25] according to the well-known Floquet theorem, its wave function can be written as $\exp(-i\epsilon_k t+ikr)u_{\epsilon_k k}(r,t)$, where ϵ_k and k are quasienergy and quasimomentum, respectively, and $u_{\epsilon_k k}(r,t)$ is periodic with respect to r and t. This makes a substantial difference.

Before we discuss the dynamical model for the BO in detail in the following sections, let us take a look at a special example of the influence of the high-frequency dipole field on the WSL. Supposing the field $F(t)=F+F_1\cos(\omega t)$ and $eFd=\omega$, i.e., the ac field is exactly resonant with the WSL, the quasienergy can be obtained analytically in a nearest-neighbor tight-binding model[25] as

$$\epsilon_k=\frac{\Delta}{2}J_1\left(\frac{eF_1 d}{\omega}\right)\cos(kd), \tag{5}$$

where J_1 is the first-order Bessel function of the first kind. Thus each level of the original WSL may broaden into a quasienergy band with a width of $\Delta J_1(F_1/F)$, and the originally localized Wannier-Stark states can be dynamically delocalized. This is essentially different from an understanding based on the static approximation, where neither broadening (without scattering) nor the DDL exists. Furthermore, if the broadening width here is compared to the swinging amplitude in Ref. 20, then it is not dependent on the Wannier-Stark index, but proportional to the bandwidth Δ.

In this paper, we focus on the FWM spectra in both dc- and ac-driven superlattices, with a special emphasis put on understanding the experimental results presented by Lyssenko *et al.*[20] To our knowledge, in spite of the feasibility of the FWM technique[29] for the study of coherent phenomena,[8,9,30,31] there has been no previous theoretical work devoted to FWM spectra in such a dynamical system, though many papers have extensively studied its intraband dynamics[21] and the linear[32] interband optical properties.[33–36]

This paper is organized as below. After this introduction, we describe our theoretical model in Sec. II. The analytical results based on an ideal model are presented in Sec. III, as a guide to our numerical results shown in Sec. IV, where two situations with and without the exciton effect are thoroughly studied. Discussions and conclusions are given in Sec. V. An illustrative understanding based on the concept of the dressed WSL is presented in Appendix A, and an analytical model for solving the WSL with the exciton effect is derived in Appendix B.

II. THEORETICAL MODEL

The system we consider is a semiconductor superlattice in the presence of a static electric field F as well as a time-dependent one $F_1(t)$, both applied along the growth direction. $F_1(t)$ may simulate the weak dipole field due to the BO,[20] or represent the field brought by a free-electron laser as in most THz experiments in the superlattices.[12,26,27] In the former case, the dipole field depends critically on the excitation condition, and thus has a rather complicated time dependence. For the sake of simplicity, in this paper $F_1(t)$ is assumed to be of the same form as $F_1\cos(\omega t)$, where, if not specified, ω is taken to be the WSL spacing, $\omega_{BO}\equiv eFd$ (hereafter we will let $\hbar=1$).

In view of the fact that the ground state of excitons predominates in the FWM signals, especially when the central excitation frequency ω_0 is somewhat below E_0 (the interband transition energy in the same well) and when the excitation bandwidth is comparable to ω_0-E_0,[18] the in-plane movements of electrons in the superlattice can be neglected concerning the FWM signals in this paper. Thus the system can be modeled by a one-dimensional tight-binding two-

band Hamiltonian, which is expressed in the Bloch representation as

$$H=H_0+H_F+H_c+H_r, \tag{6}$$

$$H_0=\sum_{i=e,h;k}\left[E_i-\frac{\Delta_i}{2}\cos(kd)\right]a^{\dagger}_{i,k}a_{i,k}, \tag{7}$$

$$H_F=\sum_k ieF(t)(a^{\dagger}_{e,k}\partial_k a_{e,k}+a^{\dagger}_{h,-k}\partial_k a_{h,-k}) -\chi(t)(a_{h,-k}a_{e,k}+a^{\dagger}_{e,k}a^{\dagger}_{h,-k}), \tag{8}$$

$$H_c=-\frac{V_0}{N}\sum_{k,k',q}a^{\dagger}_{e,k+q}a^{\dagger}_{h,-k'-q}a_{h,-k'}a_{e,k}, \tag{9}$$

where H_0 is the unperturbed Hamiltonian, H_F includes the interaction between the electric fields and the carriers and the optical interband excitations, H_c is the Coulomb interaction between electrons and holes, and H_r denotes the relaxation process, which is characterized by a phenomenological interband dephasing rate γ_2 in the calculations. E_e (E_h) and Δ_e (Δ_h) represent the central energy and the bandwidth of the electron (hole) miniband, respectively; $a_{e,k}$ ($a_{h,k}$) is the electron (hole) annihilation operator with the Bloch wave vector k; $a^{\dagger}_{e,k}$ and $a^{\dagger}_{h,k}$ are the corresponding creation operators; V_0 is the Coulomb interaction matrix element; N is the number of periods of the superlattice; and $\chi(t)$ denotes the dipole interaction between the carrier pairs and the optical field, which is assumed to be k independent. The assumed contact Coulomb interaction potential retains the dominant part of the Coulomb interaction, which results in a single bound-state structure for excitons in the absence of the external fields.[37] This on-site Coulomb interaction model has already been adopted by other researchers.[31,35,38] As matter of fact, the long-range part of the Coulomb interaction has already been included in the dipole field due to the BO in our model.

In a two-beam (degenerate) FWM configuration,[29] the first incident laser pulse at the direction $\mathbf{k_1}$ and the second one delayed by time τ at the direction $\mathbf{k_2}$ together create a grate inside the sample, and the self-diffracted signal in the direction $\mathbf{2k_2-k_1}$ is detected as the FWM signal. The optical dipole coupling can be written as

$$\chi(t)=\frac{\chi_1(t)}{2}\exp(i\mathbf{k_1}\cdot\mathbf{r}-i\omega_0 t) +\frac{\chi_2(t)}{2}\exp[i\mathbf{k_2}\cdot\mathbf{r}-i\omega_0(t-\tau)]+\text{c.c.}, \tag{10}$$

where $\chi_i(t)$ contains the pulse shape function, which is chosen to be the Gaussian, so that $\chi_1(t)=\chi_0\exp(-\Omega^2t^2/2)$ and $\chi_2(t)=\chi_1(t-\tau)$.

The FWM signals are calculated based on the semiconductor Bloch equations,[39] which are extended to the case including the external fields.[38] The quantities of interest are the particle populations $f_{e/h,k}\equiv\langle a^{\dagger}_{e/h,k}a_{e/h,k}\rangle$ and the interband polarization $p_k\equiv\langle a_{h,-k}a_{e,k}\rangle$. Since the intraband relaxation dynamics is not included in the present paper, $f_{e,k}=f_{h,-k}\equiv f_k$. By using the Coulomb interaction within the Hartree-Fock approximation, the semiconductor Bloch equations read

$$\partial_t p_k=-i\epsilon_k(t)p_k-\gamma_2 p_k+eF(t)\partial_k p_k+i\chi^R(t)(1-2f_k), \tag{11}$$

$$\partial_t f_k=eF(t)\partial_k f_k-2\,\mathrm{Im}\{\chi^R(t)p_k^*\}, \tag{12}$$

where the energy and optical field are renormalized according to the Hartree-Fock interaction as

$$\epsilon_k(t)=\epsilon_k-2\sum_{k'}f_{k'}V_0/N =E_g-\frac{\Delta}{2}\cos kd-2\sum_{k'}f_{k'}V_0/N, \tag{13}$$

$$\chi^R(t)=\chi(t)+\sum_{k'}p_{k'}V_0/N. \tag{14}$$

Here $E_g\equiv E_e+E_h$ and $\Delta\equiv\Delta_e+\Delta_h$.

There are three types of nonlinear terms contributing to the FWM signals, namely, the Pauli blocking, the carrier energy renormalization, and the optical field renormalization. To calculate the FWM signals, it is required to expand f_k and p_k into different spatial Fourier components, and to obtain the corresponding spatial component expressions for the semiconductor Bloch equations.[40] Within the so-called χ-3 approximation, the only relevant spatial components are $p_k^{(1)}$, $p_k^{(2)}$, $f_k^{(21)}$, and $p_k^{(221)}$, and their complex conjugates, where the superscripts denote the spatial directions $\mathbf{k}_1$, $\mathbf{k}_2$, $\mathbf{k}_2-\mathbf{k}_1$, and $2\mathbf{k}_2-\mathbf{k}_1$, respectively. The total χ-3 polarization in the direction $2\mathbf{k}_2-\mathbf{k}_1$ is $p^{(221)}=\Sigma_k p_k^{(221)}$. Thus the time-resolved FWM signal is $|p^{(221)}(t)|^2$, the time-integrated FWM (TI-FWM) signal is $\int_{-\infty}^{+\infty}dt|p^{(221)}(t)|^2$, and the spectrally resolving (SR-FWM) signal is $|p^{(221)}(\omega)|^2$.

In the following calculations, for the sake of comparison, we will use the same sample parameters as in Ref. 20, i.e., $d=8.4$ nm, $\Delta=40$ meV, and $E_0=1.582$ eV. When the Coulomb interaction is introduced, we adjust E_g accordingly so as to fix E_0.

III. ANALYTICAL RESULTS

When the δ-function-like pulse is assumed for the optical excitation [i.e., in the expression for the $\chi_1(t)$, $\Omega=\infty$], the Coulomb interaction is ignored [i.e., $V_0=0$ in Eq. (9)], and the rotating-wave approximation is used for the interband optical transition, the FWM signals can be analytically evaluated so as to give insights into the numerical results in Sec. IV. By integrating the semiconductor Bloch equations for the pertinent Fourier component of populations and polarization in the moving frame[38]

$$\tilde{k}(t)=k-\int_0^t eF(t)dt, \tag{15}$$

we obtain[41]

$$p^{(22\bar{1})}_{\tilde{k}(t)}(\tau,t)=\frac{i}{4}\chi_2^2\chi_1^*\theta(t-\tau)\theta(\tau)\times e^{i\int_0^{\tau}(\epsilon_{\tilde{k}(t')}+i\gamma_2)dt'}e^{-i\int_{\tau}^{t}(\epsilon_{\tilde{k}(t')}-i\gamma_2)dt'}, \quad (16)$$

where θ is the step function. Clearly, the spectral information is entirely contained in the last exponential term on the right-hand side of the equation, which will be referred to as $I_k(t,\tau)$. By using

$$\exp(iz\sin\varphi)=\sum_{n=-\infty}^{+\infty}J_n(z)e^{in\varphi}, \quad (17)$$

we obtain

$$\epsilon_{\tilde{k}(t)}=E_g-\sum_{n=-\infty}^{+\infty}\frac{\Delta}{2}(-1)^nJ_n\left(\frac{\omega_1}{\omega}\right)\cos(kd-\omega_{BO}t+n\omega t), \quad (18)$$

$$I_k(t,\tau)=e^{-i(E_g-i\gamma_2)(t-\tau)}\prod_{n=-\infty}^{+\infty}\exp\left\{-i\frac{\Delta}{2}(-1)^nJ_n\left(\frac{\omega_1}{\omega}\right)\frac{\sin(kd-\omega_{BO}t'+n\omega t')\big|_{t'=\tau}^{t'=t}}{n\omega-\omega_{BO}}\right\}, \quad (19)$$

where ω_1 denotes the ac field intensity, equal to eF_1d. The exponential terms inside the product of Eq. (19) can be expanded again according to Eq. (17) to yield simple harmonics and the spectral information.

If $\omega_1=0$, i.e., there is no time-dependent dipole field, $\epsilon_{\tilde{k}}$ is periodic in time and so is $I_k(t,\tau)$ except for a common factor of $\exp[-i(E_g-i\gamma_2)(t-\tau)]$ for all k's. Thus the Fourier transformation of $p^{(221)}(t)$ produces the well-known WSL with an equal spacing of ω_{BO}.

For $\omega_1\neq 0$, let us examine three different cases, respectively. That is, ω_{BO}/ω is an integer p, a rational number p/q (p and q are relative primes), and an irrational number.

When $\omega_{BO}=p\omega$, a time-independent term $\epsilon_k^p\equiv-(\Delta/2)(-1)^pJ_p(\omega_1/\omega)\cos(kd)$ will emerge from $\epsilon_{\tilde{k}}$, which has the miniband dispersion modulated by $(-1)^pJ_p(\omega_1/\omega)$. Then $I_k(t,\tau)$ can be expressed as product of $\exp[-i(E_g+\epsilon_k^p-i\gamma_2)(t-\tau)]$ and a temporally periodic function. So the SR-FWM spectrum has sidebands at $E_g+n\omega$, and each of them is broadened into a continuum of the width $|\Delta J_p(\omega_1/\omega)|$. In the special case that $F_1(t)$ has the same period as the BO, the originally discrete WSL broadens, and the localized Wannier-Stark states are delocalized accordingly. The delocalization can be understood in terms of the photon-assisted[42] hopping.[43] Note that, as mentioned in Sec. I, in the full dynamical model, the broadening width, independent of the Wannier-Stark index, is proportional to the combined miniband width, and the spacing between neighboring sidebands is constant with respect to the delay time; conversely, in the static approximation, there would be no broadening without scattering, and the WSL spacing, as a periodic function of the delay time, is irrelevant to the miniband width. When the strength of the temporally periodic field satisfies the condition $J_p(\omega_1/\omega)=0$, the quasienergy band collapses, and the DL takes place.[23–25]

When $\omega_{BO}/\omega=p/q$, $\epsilon_{\tilde{k}}$ is periodic in time with the period $p\tau_{BO}=2p\pi/\omega_{BO}=2q\pi/\omega$. The sidebands occur at $E_g+m\omega_{BO}-n\omega$, and the quasienergy band is collapsed into $2q$ discrete levels, i.e., $-\omega$, $\omega(-q+1)/q,\ldots,\omega(q-1)/q$, as already found by directly solving the Schrödinger equation.[21] This corresponds to the so-called fractional WSL (see Refs. 28 and 31).

When ω_{BO}/ω is an irrational number, $\epsilon_{\tilde{k}}$ is not periodic in time, and all multiple-photon sidebands at $E_g+m\omega_{BO}-n\omega$ will in principle appear in the FWM spectrum, which, as a quasicontinuum spectrum, will exhibit some interesting patterns—the fractal structure for the WSL. Certainly, this is out of the scope of this presentation.

Figure 1 is the calculated FWM spectra at different delay times, in which a δ-pulse excitation and no exciton effect are assumed. The parameters are chosen as $\omega_{BO}=\omega=15$ meV($\tau_{BO}\approx 276$ fs) and $\omega_1=0.15\omega_{BO}$. In addition, we take a quite small dephasing rate $\gamma_2=0.05$ meV (cf. the realistic one is of the order 1 meV), corresponding to a dephasing time as long as $48\tau_{BO}$.

As expected from the above analysis, Fig. 1 verifies that the dipole field broadens the WSL into a series of continua of the width about 3 meV, evenly separated by 15 meV. The broadening depends on neither the delay time nor the

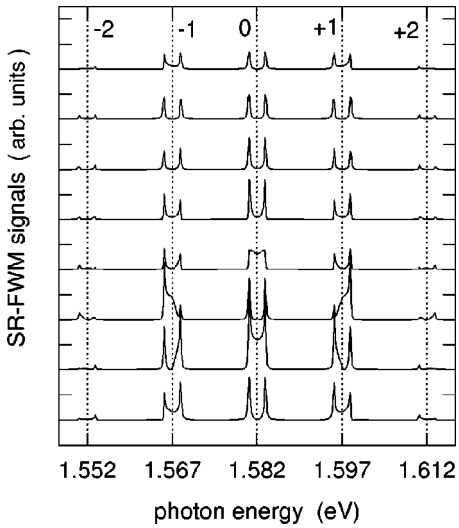

FIG. 1. SR-FWM signals for δ-pulse excitations at several delay times from 0 fs (top) to 280 fs (bottom) with 40-fs intervals, where the exciton effect is ignored. The curves are shifted vertically for clarity. The vertical dotted lines and the integers nearby label the Wannier-Stark transitions in the absence of the ac field.

Wannier-Stark index. Since the dephasing broadening here is only 0.05 meV, the broadening can be unambiguously ascribed to the DDL.

Three features on the spectral line shape are worth pointing out. First, the quasienergy band structure is clearly visible; in particular, at two edges of each continuum the signal intensity appears sharp peaks, which looks as if the WS level were split. This results from the singularity of the density of states at the center and the edges of the Brillouin minizone. Second, the spectral line shape is relevant to the delay time because of the τ-related terms in Eq. (16). Thus, when a larger dephasing rate smears out the quasienergy band structure, the variation of the FWM spectra with the delay time will look like the swinging WSL peaks. This swinging, however, differs essentially from the predictions based on the static approximation. Third, the spectra exhibit some kind of symmetry with respect to the Wannier-Stark level with index 0. These features, however, depend crucially on the negligible dephasing, the δ-function-like excitation, and the absence of Coulomb interaction.

IV. NUMERICAL CALCULATIONS

In this section more realistic situations, including the finite duration of the excitation pulses and the sufficient dephasing, will be examined and evaluated. The exciton effect is ignored at first, and taken into account in Sec. IV B. The semiconductor Bloch equations are numerically integrated in the moving frame over a period of time long enough to obtain the FWM spectra quantitatively. In the following, if not specified particularly, Ω is set to be 9 meV (corresponding to the pulse full width about 146 fs), and the central frequency of the excitation is taken from the experiment, $\omega_0 = 1.5765$ eV,[20] a little below E_0, the energy of the zeroth Wannier-Stark level.

A. Without exciton effect

The SR-FWM signals in the first BO period are displayed in Fig. 2, in which $\gamma_2 = 0.6$ meV ($T_2 \approx 1.1$ ps), $\omega_1 = 0.1\omega_{BO}$, and other parameters are as given previously. The three features on the line shape in the FWM spectrum mentioned above have been drastically changed upon using more realistic parameters. The quasienergy band structure, as clearly seen in Fig. 1, is now blurred by the larger dephasing rate, though, at certain delay times, peak splitting can still be observed. While the spectra remain delay time dependent, the peak oscillation with the delay time deviates obviously from a simple harmonic behavior. The symmetry shown in Fig. 1 is entirely broken. Similar to the ideal situation, however, the swinging range and splitting magnitude, insensitive to the Wannier-Stark indices, approximate the quasienergy bandwidth ($\approx$2 meV). Even the peak associated with the zeroth Wannier-Stark transition is subject to such swinging and splitting.

Strictly speaking, the peaks are no longer equally separated. In contrast to the static approximation, which predicts that the WSL would be always evenly spaced without the exciton effect, as shown in Fig. 2, the WSL is somewhat destroyed by the dynamical field.

An interesting feature in Fig. 2, also unexpected from the static theory, is the finite intensity at the peaks ± 2, which are

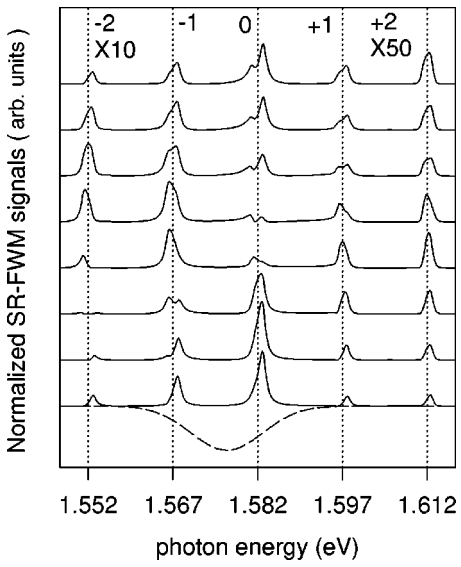

FIG. 2. SR-FWM signals at different delay times from 0 fs (top) to 280 fs (bottom) with 40-fs intervals for the finite excitation pulse width ($\approx$146 fs), where the dephasing rate is 0.6 meV. For clarity, the curves are vertically shifted and normalized (divided by the TI-FWM signals), and the peaks at ± 2 are enlarged. The excitation spectrum is reversed and plotted with a long-dashed line. The vertical dotted lines and the nearby integers label the Wannier-Stark transitions.

well beyond the excitation energy range. Regarding the fact that the higher the Wannier-Stark index p, the smaller the overlap factor of $|J_p(\Delta/(2\omega_{BO}))|^2$ which is directly related to the FWM signal intensity at the pth peak, this feature seems even more amazing.

This feature can be comprehended in the full dynamical model. Due to the DDL, electrons can hop to their neighboring Wannier-Stark states by absorbing or emitting a photon, which leads to signals out of the excitation energy window, until the coherence is lost. To verify this, we have calculated the normalized SR-FWM signals at zero delay time for several dipole-field strengths as shown in Fig. 3(a). The relative ac field strength ω_1/ω_{BO} for calculation takes the values of 0, 0.1, 0.2, and 3.8317 (the first root of J_1), with other parameters kept as in Fig. 2. When there is no dynamical field, significant signals only exist at the Wannier-Stark transitions with indices of 0 and ± 1, which, as expected, locate within the pulse excitation window and are favored by the larger overlap factors. Since in the absence of the ac field the broadening results solely from the dephasing, the FWM signals are exactly of Lorentzian shape. When the dynamical field F_1 grows, the peaks are broadened further and split by DDL, with the line shapes deviating from the Lorentzian significantly. The DDL reduces the FWM peak at index 0 notably; at the same time, it evidently enhances the peaks at ± 1 and at ± 2.

When the field approaches the first root of the Bessel function ($F_1 = 3.8317F$), DL occurs. Then the peak with index 0 is almost restored to the one without the ac field, and the resumed Lorentzian line shapes for the peaks are narrower than the signals when DDL occurs. The peaks at ± 1 are nearly invisible because they are out of phase at zero delay time, but not so at other delay times. Most notably, compared with the case without the high-frequency field, the

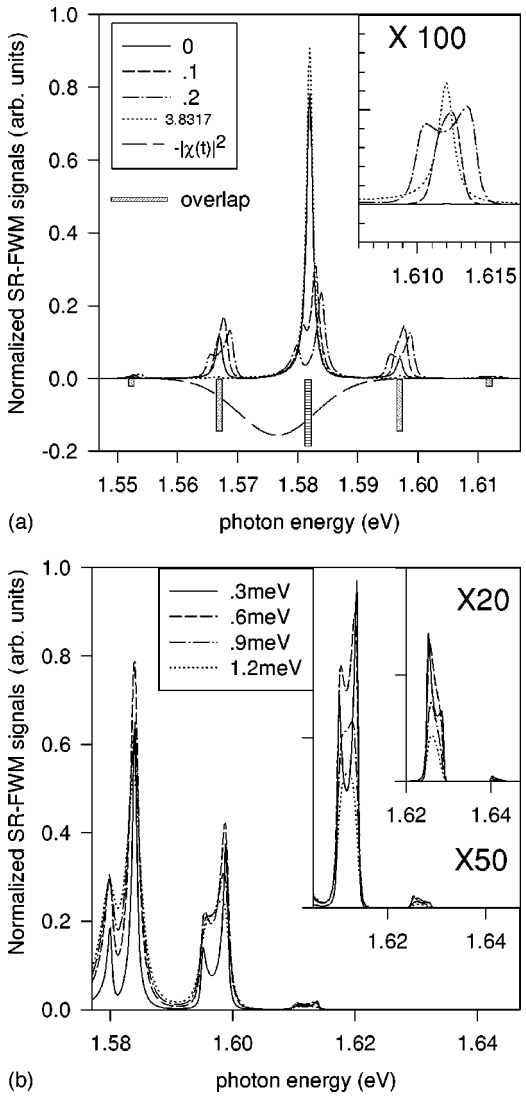

FIG. 3. The normalized SR-FWM signals at zero delay time (a) for different field intensities ($\gamma_2 = 0.6$ meV), and (b) for different dephasing rates ($\omega_1/\omega_{BO} = 0.15$). The filled bar denotes the overlap factor at each Wannier-Stark transition in a vanishing ac field. The insets on the top right in both (a) and (b) show the enlarged signals with the Wannier-Stark index $+2$, and, as also shown in (b), the $+3$ peaks are further enlarged 20 times. The reversed excitation spectrum (long-dashed line) is shown for reference.

peaks at ± 2 remain finite, indicating a finite probability of the photon-assisted transitions among the WSL even when DL occurs. Clearly, DL is in nature different from the Wannier-Stark localization, and the DL spectrum cannot be interpreted within the static approximation. It is clear from the discussions above that, owing to the applied high-frequency field, the FWM peaks associated with the Wannier-Stark transitions beyond the excitation window may be experimentally detected.

It takes time for photon-assisted transitions to occur between Wannier-Stark levels. Thus, the longer the relaxation time, the farther the electron's hopping and the stronger the out-of-window peaks. This anticipation is confirmed by the calculations with various dephasing rates such as 0.3, 0.6, 0.9, and 1.2 meV. As shown in Fig. 3(b), with decreasing γ_2, the peak with a low Wannier-Stark index (0 or $+1$), which is within the excitation window, is weakened, while the peak with index $+2$ or $+3$, which would vanish without the DDL effect, is strengthened.

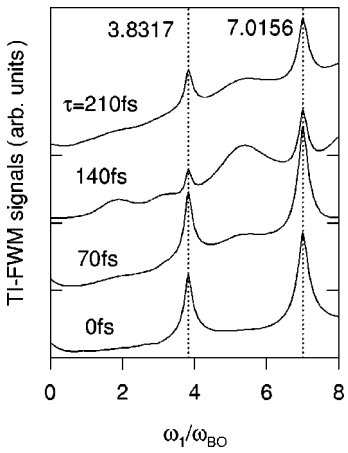

FIG. 4. TI-FWM signals vs the dynamical field strength at several delay times 0, 70, 140, and 210 fs. The curves are shifted for clarity. Except for the field strength, the parameters are the same as in Fig. 2. The numbers on the top indicate the first two nonzero roots of the Bessel function J_1 (vertical dotted lines).

In Fig. 4, TI-FWM signals at various delay times are plotted as functions of the dynamical field intensity. Sharp peaks are at such field intensities where DL occurs, because the collapse of the quasienergy band makes the contributions from all the quasimomentum states interfere constructively [see Eq. (16)]. This finding demonstrates that the TI-FWM technique is feasible to study the DL phenomena. There are also peaks of the TI-FWM signals at $F_1 = 0$ due to the Wannier-Stark localization. These peaks are much weaker than those due to DL, particularly for longer delay times. This suggests that an intense and coherent high-frequency field is able to synchronize the motion of electrons and thus to enhance the coherent signals. The synchronization may likewise be the origin of the overall signal enhancement with increasing dipole field. Some extra structures can also be observed in the TI-FWM spectra as shown in Fig. 4, but they are sensitive to the delay time and less pronounced.

With the exciton effect taken into account, Ray and Basu[33] predicted the enhancement of the interband opacity when DL occurs. Our calculations show that this enhancement is possibly not related to the exciton effect, but rather to the constructive interference. In fact, our following calculation will show that this enhancement is somewhat handicapped by the exciton effect.

B. With exciton effect

It is well known that exciton states play a key role in semiconductor interband optics. Now we examine their influence on the FWM spectra of the dynamically driven semiconductor superlattice. A basic fact that Coulomb interaction makes the WSL no longer equally spaced, as shown in this subsection and in Appendix A, will mainly determine the dynamical process of the excitonic Wannier-Stark levels (XWSL's). The energies of the XWSL's in this paper are evaluated according to an analytical expression [Eq. (B4)], which is derived in Appendix B with a special contact Coulomb potential model.

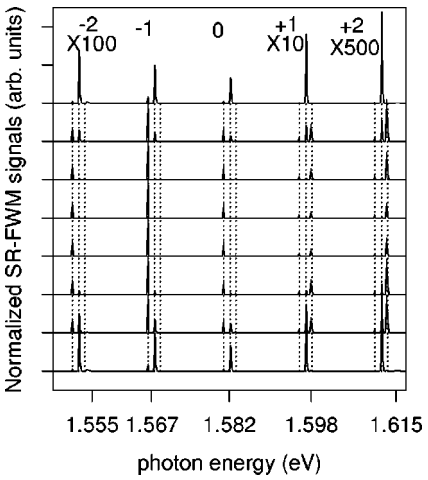

FIG. 5. Excitonic SR-FWM signals at different delay times from 0 fs (top) to 280 fs (bottom) with 40-fs steps, for the δ-pulse excitation. The signals are normalized, scaled by different factors as shown in the figure, and shifted for clarity. The vertical dotted lines designate the spectral positions calculated with the dressed WSL model in Appendix A. The energies of the XWSL's without the dynamical field are labeled below the bottom line.

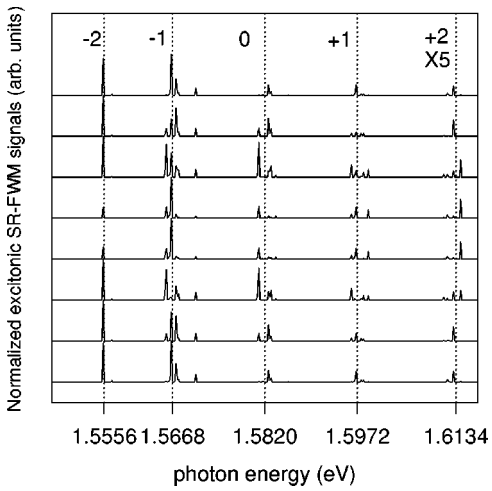

FIG. 6. Excitonic SR-FWM signals similar to those in Fig. 5, with different parameters given in the text. The vertical dotted lines here represent the spectral positions of the XWSL's without the dynamical field.

In our following calculations, the contact Coulomb potential V_0 is taken to be 10 meV, and the other parameters are kept the same as in Fig. 1, if not specified. In all cases, E_g is adjusted in order to fix the energy of the zeroth XWSL E_0^X at the experimental value 1.582 eV.

Figure 5 demonstrates the delay-time dependence of the SR-FWM signals within a BO period. Compared with the case without the exciton effect as shown in Fig. 1, the symmetry in the FWM spectra now is absent, the transitions with high Wannier-Stark indices (± 2) diminish obviously, and each XWSL is split into a group of discrete lines, whose relative intensity varies with the delay time. Most strikingly, the groups are evenly separated by the frequency of the ac field, i.e., $\omega = \omega_{BO} = 15$ meV, though the original XWSL's are unequally spaced.

The discrete spectrum and the diminished higher peaks indicate that the DDL effects are significantly weakened by the exciton effect. Two intuitive pictures may help us to understand qualitatively why the DDL is reduced. One is that the attraction between electrons and holes tends to prevent the electrons from being delocalized by the ac field. The other is that the unequal spacing between the XWSL's makes the photon-assisted hopping more difficult.

To understand better the reduced DDL due to the exciton effect, a concept of the dressed WSL is invoked, by which the coupled system of the XWSL's with the dipole field is transformed into a one-dimensional tight-binding model, where the nth site energy is $E_n^X - n\omega$, and the coupling between the nearest sites is related to the dynamical field (see Appendix A for details). Calculation based on Eq. (B4) shows that the energy separations between neighboring XWSL's with indices lower than ± 3 deviate from $eFd = 15$ meV significantly, while the XWSL's with higher indices form an almost perfect WSL, as if there were no Coulomb interaction. So, if XWSL's with lower indices are compared to some kind of imperfection in the whole WSL, the states localized around these ''impurities'' may be discrete. If so, the optical spectrum will exhibit a discrete line structure because bound-exciton states have much larger oscillator strengths than continua.

The success of such a simple model is remarkable. The quasienergies of the localized states, calculated with the dressed WSL model (vertical dotted lines in Fig. 5), are excellently consistent with the spectral lines calculated with the full dynamical model; at the same time, the relative strengths of the lines within a group are also well explained by this model, i.e., bound states with larger probability distributed in sites with lower XWSL indices have larger oscillator strengths. As shown in Appendix A, the multiple-photon sidebands of these bound states also appear in optical spectra due to their quasienergy nature, which is why the groups of lines in the FWM spectra are equally separated by the ac frequency.

This understanding is further supported by the calculation as shown in Fig. 6. In this figure, we have set $\omega_{BO} = 14.37$ meV and $\omega = 15.21$ meV, with other parameters unchanged. In this carefully chosen situation, the spacing between XWSL's with indices 0 and ± 1 is resonant with the ac field, while the remote levels are spaced almost equally by ω_{BO}. The resonance is expected to delocalize electrons among states with lower Wannier-Stark indices which have large oscillator strength. An enhancement of the DDL effect is indeed realized. Compared with Fig. 5, the number of lines in a group increases, the spectrum looks more like a continuum, and the signals with high Wannier-Stark indices (± 2) are strengthened. Again, all these features are well reproduced by calculations based on the dressed WSL model in Appendix A.

In general, the DDL is reduced by the exciton effect, particularly by the unequal spacing between XWSL's. This reduction, however, can be alleviated by adjusting the static field strength to achieve equal spacing for some Wannier-Stark states with low indices, and simultaneously tuning the ac field to realize the resonance. We think that the combination of a static and a time-periodic field does provide a flexible way to engineer the XWSL's dynamics.

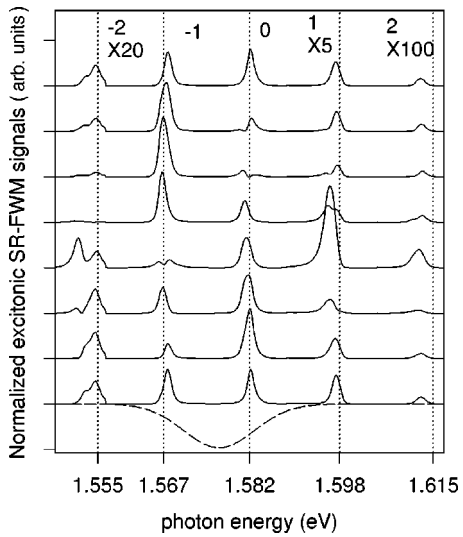

FIG. 7. Exciton SR-FWM signals with a dephasing rate of 1.2 meV and an excitation pulse width of 146 fs. The curves are plotted in a similar way to those in Fig. 2. The vertical dotted lines and the *x*-axis labels designate XWSL's without an ac field.

In Figs. 5 and 6, the relative strengths of the spectral lines in each group vary with the delay time, so it is expected that the discrete spectrum might be blurred into broad peaks with varying shapes when sufficient dephasing is introduced. Figure 7 displays the results calculated with $\Omega=9$ meV, $\omega_1=0.1\omega_{BO}$, $\gamma_2=1.2$ meV, and other parameters the same as in Fig. 5. The following features are observed which are absent in the static approximation. First, peak swinging exists for all Wannier-Stark transitions with low indices, in particular including the zeroth. Second, there seems to be no simple relation between the Wannier-Stark index and the swinging amplitude as well as swinging phase. Third, some of the peaks are still split at certain delay times, and the structures in Fig. 5 are not fully smeared out.

The excitonic TI-FWM signals are plotted in Fig. 8 as functions of the dynamical field's strength. As in the case without the exciton effect, the signals are at their peaks when the DL occurs. The peaks, however, are not so sharp as in Fig. 4, and their positions deviate slightly from the roots of the Bessel function. This effect has to be ascribed to the exciton effect since all parameters but V_0 and E_g are identical to those in Fig. 4. The exciton effect also results in extra peaks and shoulders on both sides of the DL peaks, which was not revealed in Ref. 33 because of its too simple model. But it has also been reported that the oscillator strength of the exciton states reaches a maximum when the DL takes place.

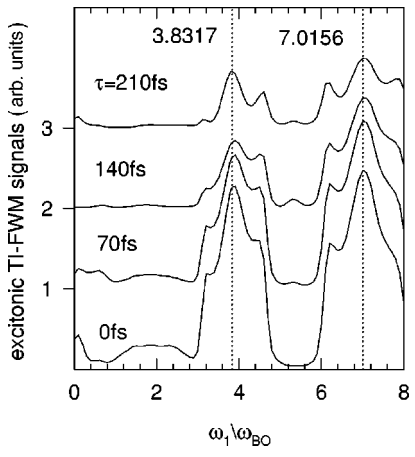

FIG. 8. Excitonic TI-FWM signals vs the dynamical field intensity at different delay times. Parameters are the same as in Fig. 7, except for $\gamma_2=0.6$ meV. The roots of $J_1(x)$ are denoted by the dotted lines.

V. DISCUSSIONS AND CONCLUSIONS

In summary, based on the full dynamical model, we have calculated the FWM signals from a semiconductor superlattice in the presence of both static and time-dependent electric fields. When the exciton effect is negligible, an ac field with a frequency identical to the BO frequency dynamically delocalizes the otherwise localized Wannier-Stark electrons, and the FWM spectra exhibit a set of equally spaced continua in the coherent limit, reflecting the quasienergy miniband structure in the temporally periodic system. With realistic dephasing, the quasienergy structures are blurred to broad peaks, which swing in the delay-time domain with varying non-Lorentzian lineshapes. The peaks may even be split at certain delay times. The width of the continua, the splitting magnitude, and the swinging range are not dependent on the Wannier-Stark index, but are proportional to the combined miniband width and to the ac field strength, provided the ac field is weak relative to the dc field. The DDL also induces signals well beyond the excitation energy window. When the ac field satisfies the condition for the dynamical localization, the spectra become similar to those in the static field, but the out-of-window signals survive.

When the exciton effect is taken into account, the XWSL's are unequally spaced, and the DDL effects are weakened by the Coulomb binding. The dynamical excitonic FWM spectra consist of groups of discrete lines, reflecting the localization nature of the bound excitonic states. These groups are evenly separated by the frequency of the ac field, exhibiting a typical characteristic of the quasienergy states in periodically driven systems. The homogeneous broadening smears out the discrete line structures, and makes the spectra similar to those without the exciton effect.

When DL occurs, the TI-FWM signals reach their maxima, and the coherent motion of electrons are synchronized. The exciton effect blurs the peaks slightly, and induces richer structures.

We have tried various values for these parameters, such as the pulse duration and the central frequency, the dephasing rate, the electric-field strengths, the miniband width, etc. The essential features presented above remain in all situations, though the quantitative behaviors of the signals are rather sensitive to the parameters used.

Treating the high-frequency field as a quasistatic one will lead to qualitatively different results from those mentioned above; in particular, it will lead to the delay-time-dependent spacing for WSL in the FWM spectra. Since several key features predicted with the full dynamical model were not observed in the experiment.[20] We think that the experimental results could not be simply attributed to a time-periodic dipole field associated with the BO in real space, and the direct

measurement of the spatial BO is still a challenge for experimentalists. It is also very interesting to explain the phenomena reported in Ref. 20 within the full dynamical theory, and further experiments perhaps are needed.

ACKNOWLEDGMENTS

One of the authors (R.B.L.) thanks Dr. K. Chang, Professor K. Leo, Professor X. G. Wu, and Professor X. G. Zhao for their stimulating discussions and valuable comments. Support from the National Science Foundation of China and the QiuShi Science and Technology Foundation of Hong Kong are gratefully acknowledged.

APPENDIX A: DRESSED WANNIER-STARK LADDER

In this appendix, we will illustrate the DDL of electrons in both dc- and ac-driven superlattices by the concept of the ''dressed WSL,'' which is in analogy to the concept of the ''dressed atom'' in investigating the coupled system of an atom with a strong nearly resonant optical field. In the present situation, the atomic levels are replaced by the WSL or XWSL's, and the dynamical electric field $F_1(t)$ plays the role of the optical field.

Again, we first consider the case without the exciton effect, which allows an analytical analysis. With the summation relations of Bessel functions, the tight-binding Hamiltonian of the driven superlattice can be written in the Wannier-Stark representation as

$$H=\sum_{n=-\infty}^{+\infty}\{[E_n+n\omega_1\cos(\omega t)]a_n^{\dagger}a_n + \chi(t)a_n^{\dagger}(a_{n+1}+a_{n-1})\}, \tag{A1}$$

where n is the Wannier-Stark index, $E_n=n\omega_{BO}$ is the corresponding energy, and

$$\chi(t)\equiv\Delta\omega_1\cos(\omega t)/(4\omega_{BO})\equiv\chi\cos(\omega t), \tag{A2}$$

which couples the nearest Wannier-Stark states. Suppose the dressed states are superposed by the Wannier-Stark states

$$|\psi\rangle=\sum_n c_n|n\rangle; \tag{A3}$$

the expansion coefficients c_n's satisfy the time-dependent Schrödinger equation

$$i\partial_t c_n=[E_n+n\omega_1\cos(\omega t)]c_n+\chi(t)(c_{n+1}+c_{n-1}). \tag{A4}$$

When the ac field is not too strong and its frequency is nearly resonant with the spacing of the WSL, the rotating-wave approximation (RWA) is well justified, and the off-resonant terms can be dropped out. Then, with the transformation

$$c_n=\tilde{c}_n\exp(-in\omega t), \tag{A5}$$

a stationary equation can be obtained,

$$i\partial_t\tilde{c}_n=-n\Delta_f\tilde{c}_n+\chi(\tilde{c}_{n+1}+\tilde{c}_{n-1})/2, \tag{A6}$$

where $\Delta_f\equiv\omega-\omega_{BO}$ is the detuning.

When the detuning is nonzero, the eigensolution of Eq. (A6) is just the well-known localized Wannier-Stark wave function, and the coefficients for the pth eigenstate are $\tilde{c}_n^p=J_{n-p}(\chi/\Delta_f)$, with the corresponding eigenenergy $E_p=-p\Delta_f$. The dressed state can then be expressed as

$$|\psi_p(t)\rangle=e^{-ip(-\Delta_f)t}\sum_n J_{n-p}\left(\frac{\chi}{\Delta_f}\right)e^{-in\omega t}|n\rangle, \tag{A7}$$

with the quasienergy $-p\Delta_f \bmod \omega$. Similar to the Rabi splitting, here the nth level in the WSL, E_n, is split into a further miniladder as $E_n-p\Delta_f$, $(p=0,\pm1,\pm2,\ldots)$. That is, the original WSL is dressed by the dynamical field. Owing to the nonzero detuning, electrons cannot absorb or emit a real photon, and therefore cannot be delocalized by the dynamical field. The larger the detuning and/or the weaker the ac field, the more the quasienergy states will be localized [see Eq. (A7)]. In optical experiments, in principle, lines at $E_n-p\Delta_f$ are observable, with the oscillator strengths proportional to $J_{n-p}^2(\chi/\Delta_f)J_n^2(\Delta/2\omega_{BO})$, and some fascinating patterns in the spectrum can be expected.[28,31]

When the ac field is exactly resonant with the ladder, Eq. (A6) is identical to the equation for a free electron in a tight-binding periodic potential. The solution is simply the Bloch wave $|\psi_k(t)\rangle=e^{-i\tilde{\epsilon}_k t}\Sigma_n e^{inkd}|n\rangle/\sqrt{N}$, and the $\tilde{\epsilon}_k=-\chi\cos(kd)$ forms a quasienergy band. In this case the electrons are dynamically delocalized, and the dressed WSL evolves into a set of continua equally spaced by ω_{BO}.

The quasienergy bandwidth, $2\chi=(\Delta/2)(\omega_1/\omega_{BO})$, increases monotonically with the strength of the ac field, so the DL cannot be predicted within the RWA. In fact, the rigorous solution for the quasienergy dispersion, $\tilde{\epsilon}_k=-\Delta J_1(\omega_1/\omega_{BO})\cos(kd)/2$, agrees with the RWA result only in the weak ac field limit. Therefore, it is the off-resonant terms neglected in the RWA that are responsible for the DL. On the other hand, when ω_{BO} equals a multiple of ω, the exact solution predicts that there exist both DDL and DL owing to the multiple-photon resonance, but they are absent in the RWA. In a word, the RWA works only when both the weak-field limit and the nearly resonant limit are satisfied.

Now we consider the case with the exciton effect. Owing to the Coulomb interaction, the XWSL's are unequally spaced, the coupling matrix element χ generally depends on the index of the XWSL's, and the hopping integral induced by the dynamical field is not necessarily limited to between nearest neighbors. The latter two effects, however, can be ignored since the dynamical dipole field is normally quite weak compared to the static one.

Subject to the restriction of the RWA, i.e., in the weak and near-resonant dynamical field limit, similar to the procedures taken above, we obtain

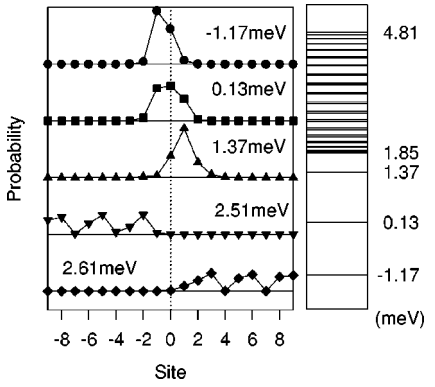

FIG. 9. Quasienergy levels (right panel) and the electron probability distributions for several quasienergy states (left panel) based on the dressed WSL model. Parameters are the same as in Fig. 5.

$$i\partial_t \tilde{c}_n = (E_n^X - n\omega)c_n + \chi(\tilde{c}_{n+1} + \tilde{c}_{n-1})/2, \qquad \text{(A8)}$$

where E_n^X stands for the energy of the excitonic Wannier-Stark level with the index n. With the XWSL's calculated from Eq. (B4), for a given ac field, the energy spectrum and wave functions can be readily solved by numerically diagonalizing Eq. (A8).

The equation above is equivalent to the equation of motion for an electron in a tight-binding lattice with some central sites occupied by ''impurities,'' considering the fact that the Coulomb interaction only affects XWSL's with low indices. Thus, for a weak and nearly resonant dynamical field, by mapping the dynamical XWSL system to the impurity band structure, we can understand that the dynamical XWSL spectrum is just a continuum plus a few discrete levels. It should be pointed out that the number of the discrete states and the localization length are determined not only by E_n^X, but also by the hopping integral χ, which can be manipulated by the ac field strength. So the localization can be controlled to some extent, as proclaimed by Holthaus and co-workers.[44]

To verify the above arguments, with the same parameters as in Fig. 5, a model calculation has been carried out in a lattice of 41 sites (levels), in which the site energies are calculated according to Eq. (B4), with E_0^X taken as the energy zero point. As shown in Fig. 9, three levels are well below a set of dense levels. These three split-off states are localized around the central ''impurities;'' other states extend to remote end sites and distribute within a quasienergy band with a width of 2.96 meV, agreeing well with that evaluated without the exciton effect, i.e., $\Delta J_1(\omega_1/\omega_{BO}) \approx 3$ meV.

Only those states with a finite distribution probability at Wannier-Stark states with low indices can contribute substantially to optical signals. For parameters used in Fig. 9, there are three such states, which are just the discrete ones. Thus the transitions at $n\omega + E_i^b$ $(n = 0, \pm 1, \pm 2, \ldots)$ may be observed in the spectra, where E_i^b $(i = 1,2,3)$ are the quasienergies of the discrete levels, with the intensity proportional to $|\tilde{c}_n^i J_n(\Delta/2\omega_{BO})|^2$. Both the positions and the relative strengths of the spectral lines according to this simple model agree excellently with the numerical results in Fig. 5. This means that the discrete line structure in the

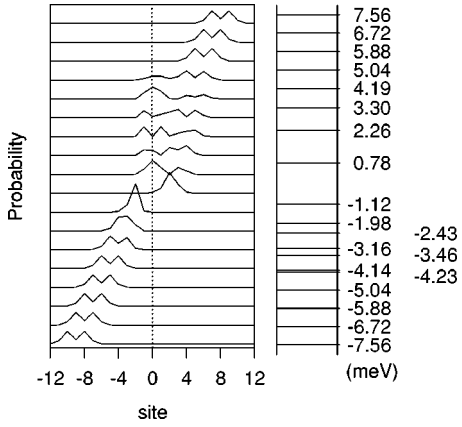

FIG. 10. Electron probability distributions (left panel) and quasienergies (right panel) based on the dressed WSL model. Parameters are the same as in Fig. 6.

FWM spectra are quite similar to atomic Rabi splitting. Note that although XWSL's with low indices are not equally spaced, the separations between neighboring groups of lines are all the same, and equal to the frequency of the ac field, ω.

As a further check of the model, the quasienergy spectrum and the wave functions based on Eq. (A8) with the parameters in Fig. 6 are calculated as shown in Fig. 10. Since now the ac field is not resonant with XWSL's at remote sites, the energies at these remote sites are not equal, but form a ladder with an approximate separation as $\omega - \omega_{BO}$; the impurity sites around site 0, however, are near degenerate due to the deliberately chosen parameters. Thus the wave functions corresponding to those ''normal'' XWSL's are well localized and similar to the Wannier-Stark states, while the states around the zeroth site tend to extend to some extent, perturbing more neighbor states as compared to Fig. 9. In other words, the DDL effect is somehow recovered by the resonance. Again, the positions and strengths of the signal lines in Fig. 6 are well reproduced by the results based on the ''dressed'' model here. From the discussions above, we are sure that it is mainly the unequal spacing of the XWSL's that is responsible for the discrete FWM spectra and the reduction of the DDL when Coulomb interaction is included.

APPENDIX B: EXCITONIC WANNIER-STARK LEVELS

In this appendix, by using the contact Coulomb potential, we will derive an analytical expression for the XWSL's in a nearest-neighbor tight-binding model in the presence of a static electric field. The single-particle Hamiltonian in the Wannier representation $\{|p\rangle\}$ is

$$H^X = -\frac{\Delta}{4} a_p^\dagger (a_{p+1} + a_{p-1}) + (E_g + peFd) a_p^\dagger a_p - V_{p,p'} a_p^\dagger a_{p'}, \qquad \text{(B1)}$$

where $V_{p,p'}$ is the Coulomb interaction matrix element. With the transformation $|n\rangle = J_{p-n}(\Delta/2eFd)|p\rangle$, the Hamiltonian can be written in the Wannier-Stark representation $\{|n\rangle\}$ as

$$H^X = E_n a_n^\dagger a_n - \sum_{p,p'} V_{p,p'} J_{p-n}(\alpha) J_{p'-n'}(\alpha) a_n^\dagger a_{n'}, \quad \text{(B2)}$$

where $E_n \equiv E_g + neFd$ and $\alpha \equiv \Delta/2eFd$. The eigenequation for the coefficients C_n then is

$$(E_n - E^X) C_n = \sum_{p,p',n'} V_{p,p'} J_{p-n}(\alpha) J_{p'-n'}(\alpha) C_{n'}. \quad \text{(B3)}$$

In general, the energy of an XWSL E^X has to be determined by numerical diagonalization. However, for the special contact potential, i.e., $V_{p,p'} = V_0 \delta_{p,0} \delta_{p',0}$, the variables can be separated, and E^X can be obtained analytically from

$$1 = \sum_{n=-\infty}^{+\infty} V_0 J_n^2(\alpha)/(E_n - E^X). \quad \text{(B4)}$$

*Electronic address: rbliu@red.semi.ac.cn

[1] F. Bloch, Z. Phys. **52**, 555 (1928).
[2] C. Zener, Proc. R. Soc. London, Ser. A **145**, 523 (1932).
[3] G. H. Wannier, Phys. Rev. **117**, 432 (1960).
[4] J. Zak, Phys. Rev. Lett. **20**, 1477 (1968).
[5] For a recent review, see, e.g., F. Rossi, in *Theory of Transport Properties of Semiconductor Nanostructures*, edited by E. Schoell (Chapman & Hall, London, 1997), Chap. 1, and references therein.
[6] E. E. Mendez, F. Agullo-Rueda, and J. M. Hong, Phys. Rev. Lett. **60**, 2426 (1988).
[7] P. Voisin, J. Bleuse, C. Bouche, S. Gaillard, C. Alibert, and A. Regreny, Phys. Rev. Lett. **61**, 1639 (1988).
[8] J. Feldmann, K. Leo, J. Shah, D. A. B. Miller, J. E. Cunningham, T. Meier, G. von Plessen, A. Schulze, P. Thomas, and S. Schmitt-Rink, Phys. Rev. B **46**, 7252 (1992).
[9] P. Leisching, P. Haring Bolivar, W. Beck, Y. Dhaibi, F. Brüggemann, R. Schwedler, K. Kurz, K. Leo, and K. Köhler, Phys. Rev. B **50**, 14 389 (1994).
[10] T. Dekorsy, P. Leisching, K. Köhler, and H. Kurz, Phys. Rev. B **50**, 8016 (1994).
[11] C. Waschke, H. G. Roskos, R. Schwedler, K. Leo, H. Kurz, and K. Köhler, Phys. Rev. Lett. **70**, 3319 (1993).
[12] K. Unterrainer, B. J. Keay, M. C. Wanke, S. J. Allen, D. Leonard, G. Medeiros-Ribeiro, U. Bhattacharya, and M. J. W. Rodwell, Phys. Rev. Lett. **76**, 2973 (1996).
[13] Q. Niu, X.-G. Zhao, G. A. Georgakis, and M. G. Raizen, Phys. Rev. Lett. **76**, 4504 (1996).
[14] M. B. Dahan, E. Peik, J. Reichel, Y. Castin, and C. Salomon, Phys. Rev. Lett. **76**, 4508 (1996).
[15] L. Esaki and R. Tsu, IBM J. Res. Dev. **14**, 61 (1970).
[16] M. M. Dignam and J. E. Sipe, Phys. Rev. Lett. **64**, 1797 (1990).
[17] G. Bastard and R. Ferreira, in *Spectroscopy of Semiconductor Microstructures*, Vol. 206 of *NATO Advanced Study Institute, Series B: Physics*, edited by G. Fasol and A. Fasolino (Plenum, New York, 1989), p. 333.
[18] M. M. Dignam, J. E. Sipe, and J. Shah, Phys. Rev. B **49**, 10 502 (1994).
[19] A. M. Bouchard and M. Luban, Phys. Rev. B **52**, 5105 (1995).
[20] V. G. Lyssenko, G. Valusis, F. Löser, T. Hasche, K. Leo, M. M. Dignam, and K. Köhler, Phys. Rev. Lett. **79**, 301 (1997).
[21] M. Holthaus and D. W. Hone, Philos. Mag. B **74**, 105 (1996), and references therein.
[22] A. A. Ignatov and Y. A. Romanov, Phys. Status Solidi B **73**, 327 (1976); D. H. Dunlap and V. M. Kenkre, Phys. Rev. B **34**, 3625 (1986).
[23] M. Holthaus, Phys. Rev. Lett. **69**, 351 (1992).
[24] M. Holthaus and D. W. Hone, Phys. Rev. B **47**, 6499 (1993).
[25] J. Zak, Phys. Rev. Lett. **71**, 2623 (1993).
[26] B. J. Keay, S. J. Allen, Jr., J. Galán, J. P. Kaminski, K. L. Campman, A. C. Gossard, U. Bhattacharya, and M. J. W. Rodwell, Phys. Rev. Lett. **75**, 4098 (1995).
[27] B. J. Keay, S. Zeuner, S. J. Allen, Jr., K. D. Maranowski, A. C. Gossard, U. Bhattacharya, and M. J. W. Rodwell, Phys. Rev. Lett. **75**, 4102 (1995).
[28] X.-G. Zhao and Q. Niu, Phys. Lett. A **191**, 181 (1994); X.-G. Zhao, R. Jahnke, and Q. Niu, *ibid.* **202**, 297 (1995).
[29] T. Yajima and Y. Taira, J. Phys. Soc. Jpn. **47**, 1620 (1979).
[30] G. von Plessen and P. Thomas, Phys. Rev. B **45**, 9185 (1992).
[31] W.-X. Yan, X.-G. Zhao, and H. Wang, J. Phys.: Condens. Matter **10**, L11 (1998).
[32] If the time-dependent field is considered as an optical field, then the so-called linear optical dynamics is actually a nonlinear one. We use the words ''linear'' and ''nonlinear'' in a sense that the driving fields are not regarded as optical fields.
[33] P. Ray and P. K. Basu, Phys. Rev. B **50**, 14 595 (1994).
[34] T. Meier, F. Rossi, P. Thomas, and S. W. Koch, Phys. Rev. Lett. **75**, 2558 (1995).
[35] T. Meier, G. von Plessen, P. Thomas, and S. W. Koch, Phys. Rev. B **51**, 14 490 (1995).
[36] K. Johnsen and A.-P. Jauho, Phys. Status Solidi B **204**, 55 (1997).
[37] I. Egri, Solid State Commun. **32**, 1017 (1979); J. Phys. C **15**, L461 (1982).
[38] T. Meier, G. von Plessen, P. Thomas, and S. W. Koch, Phys. Rev. Lett. **73**, 902 (1994).
[39] H. Haug and S. W. Koch, *Quantum Theory of the Optical and Electronic Properties of Semiconductors*, 3rd ed. (World Scientific, Singapore, 1994).
[40] M. Lindberg, R. Binder, and S. W. Koch, Phys. Rev. A **45**, 1865 (1992).
[41] K. El Sayed, D. Birkedal, V. G. Lyssenko, and J. M. Hvam, Phys. Rev. B **55**, 2456 (1997).
[42] Since the ac field is treated as a classic field, the terminology ''photon'' applied here is only for an intuitive illustration.
[43] G. Bastard and R. Ferreira, C. R. Acad. Sci. URSS **312**, 971 (1991); R. Ferreira and G. Bastard, Surf. Sci. **229**, 424 (1990).
[44] M. Holthaus, Phys. Rev. Lett. **69**, 1596 (1992); D. W. Hone and M. Holthaus, Phys. Rev. B **48**, 15 123 (1993); M. Holthaus, G. H. Ristow, and D. W. Hone, Phys. Rev. Lett. **75**, 3914 (1995).